NASA
Technical Paper 1622

AVRADCOM
Technical Report 79-46

Spur-Gear-System Efficiency at Part and Full Load

Neil E. Anderson and Stuart H. Loewenthal

FEBRUARY 1980

NASA

US ARMY AVRADCOM

NASA
Technical Paper 1622

AVRADCOM
Technical Report 79-46

Spur-Gear-System Efficiency at Part and Full Load

Neil E. Anderson
Propulsion Laboratory
AVRADCOM Research and Technology Laboratories
Lewis Research Center, Cleveland, Ohio

Stuart H. Loewenthal
Lewis Research Center
Cleveland, Ohio

National Aeronautics
and Space Administration

**Scientific and Technical
Information Office**

1980

SUMMARY

A simple method for predicting the power loss of a steel spur gearset of arbitrary geometry supported by ball bearings was developed. The method algebraically accounts for losses due to gear sliding, rolling traction, and windage and incorporates an expression for ball-bearing power loss to obtain an accurate estimate of spur-gear-system efficiency at part-load as well as full-load conditions. The analysis was compared with data from an experimental investigation. Theoretical predictions generally agreed with the test data except at low oil flow rates, where the analysis underestimated the gear-system efficiency. The theoretical sensitivity of power loss to changes in speed and load was close to that of the experimental data. A theoretical comparison of the contribution of the individual component losses relative to the total system losses indicated that losses due to rolling traction, windage, and support bearings are significant and should be accounted for in the calculation of power loss.

INTRODUCTION

Investigations of gear power loss are numerous, as evidenced by the research reported in references 1 to 5. From a practical standpoint, few, if any, of these analytical methods were intended to estimate gear efficiency accurately at less than full-load conditions. It is generally true that a gearset that is fully loaded will provide higher efficiency than one that is partially loaded. Since most machines are sized for occasional overloads, they operate at power levels substantially lower than maximum for most of their lives. With today's emphasis on reducing energy consumption of machinery, it is important to be able to accurately determine power losses at less than full-load conditions.

The basic limitation of most of the existing methods of predicting gear efficiency is that they rely solely on the selection of a coefficient of friction to determine power loss. There are various methods available for calculating this friction coefficient, each resulting in a different value. When part-load gear efficiency is calculated, the uncertainty in the selection of this coefficient may overshadow the variation in power loss at the part-load condition.

In addition, the friction coefficient, which can account for tooth sliding losses, cannot be used to calculate the rolling (or pumping) loss also present in a gear mesh. The

rolling loss is caused by hydrodynamic forces on the gear teeth. This loss, as well as gear-windage and support-bearing losses, can become a significant portion of the total mesh loss, particularly at light loads and high speeds.

The spur-gear efficiency analysis of Y. P. Chiu (ref. 5) includes the effects of both sliding and rolling in the gear mesh. Expressions for rolling and sliding losses as applied to spur-gear geometry are based on roller test data. Instantaneous values of sliding and rolling power loss are integrated over the path of contact of the gear and then averaged to obtain an average power loss. The method of reference 5 is perhaps the most thorough to date. However, it does not include gear-windage loss, support-bearing losses, or the effects of tooth load sharing across the mesh cycle. The support-bearing and rolling losses, as shown later in this report, largely dictate the part-load gear-system efficiency. Also, the expression for the coefficient of friction used in this work predicts an abnormally high loss when compared with test data.

The objectives of the analysis reported herein are (1) to provide a general method for calculating the full- and part-load efficiency of a spur-gear system of arbitrary geometry which considers losses due to gear sliding, rolling, and windage and rolling-element support-bearing losses and (2) to compare the predictions from this analysis and the analysis of reference 5 with spur-gear performance test data of reference 6.

SYMBOLS

a	semimajor width of contact ellipse, m (in.)
b	semiminor width of contact ellipse, m (in.)
C_m	dimensionless moment coefficient
$C_{m,0}$	dimensionless moment coefficient for disk of zero thickness
C_s	support-bearing basic static capacity, N (lbf)
C_1 to C_{14}	constants of proportionality; see table II
D	pitch circle diameter, m (in.)
D_a	tip diameter, m (in.)
D_m	bearing pitch diameter, m (in.)
D_o	base circle diameter, m (in.)
E	modulus of elasticity, N/m^2 (lbf/in^2)
E'	equivalent modulus of elasticity, $\dfrac{2}{\left(\dfrac{1-\gamma_g^2}{E_g}+\dfrac{1-\gamma_p^2}{E_p}\right)}$, N/m^2 (lbf/in^2)

F_H	normal applied load, N (lbf)
F_R	rolling traction force, N (lbf)
F_S	sliding force, N (lbf)
F_{ST}	static equivalent bearing load, N (lbf)
F_β	combined radial and tangential bearing load, N (lbf)
$\mathscr{F}$	face width of tooth, m (in.)
f_o	ball-bearing lubrication factor
f	coefficient of friction
G	dimensionless material parameter, $E'\alpha$
H_H	dimensionless film thickness (eq. (4))
h	isothermal central film thickness, m (in.)
h_R	thermally corrected film thickness used in rolling-traction equation (eq. (5)), m (in.)
K	constant defined in appendix C
K_f	lubricant coefficient of thermal conductivity, W/m K (Btu/hr ft ^oF)
k	ellipticity parameter, a/b
ℓ_1 to ℓ_6, $\Delta\ell$	path of contact distances defined in appendix A, m (in.)
M	bearing friction torque, N-m (in-lbf)
M_L	load-dependent part of bearing friction torque, N-m (in-lbf)
M_V	viscous part of bearing friction torque, N-m (in-lbf)
m_g	gear ratio, N_g/N_p
N	number of gear teeth
$\mathscr{N}$	efficiency, percent
n	rotational speed, rpm
P	power loss
P_{BRG}	total power loss due to rolling-element support bearings, kW (hp)
P_R	power loss due to rolling traction, kW (hp)
P_S	power loss due to tooth sliding, kW (hp)
P_W	power loss due to windage, kW (hp)
$\mathscr{P}$	diametral pitch

p	lubricant pressure, N/m^2 (lbf/in^2)
p_b	base pitch, m (in.)
Q_m	dimensionless thermal loading factor, $C_{12}\mu_0 u^2 \delta / K_f$
R	pitch circle radius or radius in general, m (in.)
R_{eq}	equivalent rolling radius, m (in.)
R_o	radius at point of contact, m (in.)
R_x	effective radius in direction of rolling, m (in.)
Re	rotating disk Reynolds number, $C_{14}\rho\omega R^2/u$
S	axial clearance between gear and housing wall, m (in.)
T	pinion torque, N-m (in-lbf)
t	disk thickness, m (in.)
U	dimensionless speed parameter, $u\eta_0/E'R_x$
u	average rolling velocity, $(V_g + V_p)/2$, m/sec (in/sec)
V	surface velocity, m/sec (in/sec)
V_S	sliding velocity, $V_g - V_p$, m/sec (in/sec)
V_T	rolling velocity, $V_g + V_p$, m/sec (in/sec)
W	dimensionless load parameter, $F_H/E'R_x^2$
w	gear contact normal load, N (lbf)
w_n	maximum normal gear tooth load, N (lbf)
w_T	transmitted load, N (lbf)
X, X_A, X_P, X_1 to X_4	path of contact distances defined in appendix A, m (in.)
y	exponent in M_L equation based on bearing geometry (eq. (15))
z	factor in M_L equation based on bearing geometry (eq. (15))
α	pressure-viscosity coefficient of lubricant, m^2/N (in^2/lbf)
β	temperature, K (^oF)
γ	Poisson's ratio
δ	temperature-viscosity coefficient, $1/K$ ($1/^oF$)
ϵ	Reynolds number exponent

θ	gear tooth pressure angle, deg
λ	dimensionless ratio of film thickness to composite surface roughness
μ, η	lubricant absolute viscosity, 10^{-3} N sec/m^2 (cP) (lbf sec/in^2)
μ_{air}	absolute viscosity of air within gearbox, 10^{-3} N sec/m^2 (cP) (lbf sec/in^2)
μ_{eq}	equivalent air-oil absolute viscosity, 10^{-3} N sec/m^2 (cP) (lbf sec/in^2)
ν	lubricant kinematic viscosity, 10^{-2} cm^2/sec (cS) (ft^2/sec)
ρ	lubricant density, kg/m^3 (lbm/ft^3)
ρ_{air}	density of air within gearbox, kg/m^3 (lbm/ft^3)
ρ_{eq}	equivalent density of air-oil mixture, kg/m^3 (lbm/ft^3)
φ_t	thermal reduction factor
ω	angular velocity, rad/sec

Subscripts:

B	bearing
g	gear
IN	input
p	pinion
R	rolling
S	sliding
TOT	total
0	ambient conditions

Superscripts:

$(\bar{})$	average value
$(\hat{})$	simplified value

ANALYSIS

The most significant sources of power loss in a spur-gear system include the gear mesh, gear windage, and support bearings. In this analysis, is assumed that the gears are made of steel and that they are jet lubricated. Furthermore, it is assumed that the gear does not come into contact with oil in the sump, so that there are no oil churning losses. Secondary losses such as momentum transfer due to oil impinging on the gear

teeth or noise generation are not treated. The windage and bearing losses can be calculated in a straightforward manner with approximate expressions. The mesh losses are more complex and are analyzed in detail.

Gear Mesh Losses

The mesh losses consist of a sliding frictional component and a hydrodynamic rolling component. The hydrodynamic rolling (or pumping) loss is the power required to entrain and compress the lubricant to form a pressurized oil film which separates the gear teeth (ref. 7). It is shown later that at light loads the rolling traction loss is a major portion of the system loss.

The calculation of sliding and rolling power loss is based on data from roller test machines, where friction due to sliding and rolling have been measured under various operating conditions. The gear contact progressing through the mesh cycle can be modeled as a constantly changing roller contact whose size, speed, and load can be calculated from involute gear geometry at the given operating conditions. The gear mesh cycle is then approximated by a large number of discrete elastohydrodynamic (EHD) contacts. The instantaneous rolling and sliding forces can be calculated for each contact, and the results integrated over the path of contact for the complete mesh cycle to obtain an average gear contact power loss.

The path of contact, the abscissa in figure 1, provides a convenient coordinate system for calculating the gear mesh losses. Figure 1 shows the assumed instantaneous gear tooth loading as three sequential pairs of gear teeth come into contact. The coordinates called out on the path of contact represent points where teeth enter or leave a mesh cycle. The path of contact is actually a line in space of fixed inclination (the pressure angle) mapped out by the instantaneous contact point between two mating gear teeth. During the mesh cycle, the load transmitted between the gears is normally carried by either one or two teeth at any one time. The average number of teeth in engagement is generally referred to as the contact ratio. Figure 1 illustrates the tooth loading pattern used in this analysis. Two teeth share the load for most of the path of contact. This gear mesh loading is based strictly on involute gear geometry with no profile modification. Dynamic loading is not included here, but its effect on efficiency is judged to be small.

Figure 2 shows the variations in the gear mesh velocities and the equivalent rolling radius as the teeth move through the mesh cycle for the spur-gear geometry used in reference 6 (see table I). The data of reference 6 are used later for comparison with the present analysis. The variations in these parameters show that the conditions in a spur-gear mesh are constantly changing, and, thus, the instantaneous losses are changing as

well. Appendix A gives the equations used to calculate points along the path of contact, gear loads, sliding velocities, rolling velocities, and values of the equivalent rolling radius.

Sliding force. - The instantaneous frictional force due to sliding of two gear teeth against each other is

$$F_S(X) = f(X)w(X) \tag{1}$$

The selection of the coefficient of friction can significantly affect the system losses, since gear tooth sliding is a major source of power loss in a loaded gearset, as shown later. For this analysis, the coefficient of friction developed by Benedict and Kelley (ref. 8) is used:

$$f(X) = 0.0127 \log \frac{\dfrac{C_1 w(X)}{\mathscr{F}}}{\mu_0 [V_S(X)] [V_T(X)]^2} \tag{2}$$

where

$$C_1 = 29.66 \text{ (SI units)}$$

$$= 45.94 \text{ (U.S. customary units)}$$

(A summary of the constants used in all equations is presented in table II.) This coefficient is probably the most accurate expression available at present for use when the true gear surface temperature is not known (ref. 7). There is no universal agreement as to the proper form of the friction-coefficient equation, particularly with regard to the effect of inlet oil viscosity. At low values of λ (ratio of minimum EHD film thickness to composite surface roughness), a significant portion of the friction is due to asperity contact. An increase in viscosity decreases the number of asperity contacts, and, thus, the friction coefficient decreases, as indicated by the Benedict and Kelley expression. If, on the other hand, full-film lubrication exists, an increase in viscosity increases the friction coefficient. As a practical matter, very few gear applications would be expected to have full-film lubrication.

Benedict and Kelley conducted their tests on rollers with an initial rms surface roughness of 0.4 micrometer (16 μin.). The gears of reference 6 (cited in this report for comparison with theory) were precision hobbed, a process that results in an rms surface roughness of approximately 0.4 micrometer (16 μin.). Since the operating speeds and values of λ in reference 6 are similar to those in the tests done by Benedict and Kelley, the friction equation (eq. (2)) should be applicable. Strictly speaking, equation (2) is valid when λ is less than approximately 2, which is the range of most gear

applications. Extending its use to systems with higher values of λ should not introduce serious errors.

The variation in coefficient of friction as determined by equation (2) for the gear geometry of reference 6 is shown in figure 2. The coefficient of friction varies along the path of contact because of the variation of the sliding velocity. Equation (2) does not predict accurate values of the friction coefficient at low sliding velocities (near the pitch point). An upper limit of $f = 0.1$ was set in the computer program. This limit should not introduce serious errors in the power loss calculation since the sliding power loss is relatively low at this point and of short duration.

Rolling force. - The calculation of rolling traction is common to bearing analysis (ref. 9), but is generally overlooked in calculations of gear power loss. The resistance a ball encounters when rolling over a lubricated bearing race is due to the hydrodynamic pressure forces that build the EHD film in the ball-raceway contact. Similar phenomena occur as two rollers roll over each other or as two gear teeth move across one another. The buildup of pressure on the rolling surfaces resists the motion of the two bodies and, therefore, absorbs power.

Experimental work conducted by Crook (ref. 10) on rolling traction in roller contacts can be used to calculate the rolling losses in a gear mesh. The rolling traction force can be expressed as

$$F_R = C_2 h_R \tag{3}$$

where

$$C_2 = 9.0\times10^7 \text{ (SI units)}$$
$$= 1.3\times10^4 \text{ (U.S. customary units)}$$

In this investigation, it is assumed that the gear contact operates principally in the viscous-elastic lubrication regime. The gear contact film thickness is calculated by the method of Hamrock and Dowson (ref. 11):

$$H_H = \frac{h}{R_x} = 2.69\ U^{0.67} G^{0.53} W^{-0.067} (1 - 0.61\ e^{-0.73k}) \tag{4}$$

(See appendix B for application of this equation to the present analysis.) At high pitch line velocities, this equation generally overestimates the actual film thickness. The reason for this is that thermal and starvation effects, which are not included in the equation, limit the buildup of the lubricating film. A thermal reduction factor φ_t developed in reference 12 (see fig. 3) is used to limit h at high speeds as follows:

$$h_R = h\varphi_t \tag{5}$$

Therefore the instantaneous rolling traction force for a gear mesh becomes

$$F_R(X) = C_2 h(X) \varphi_t(X) \mathcal{F} \tag{6}$$

Sliding and rolling power loss. - The instantaneous sliding and rolling power loss can be expressed as

$$\left.\begin{aligned} P_S(X) &= C_3 V_S(X) F_S(X) \\ P_R(X) &= C_3 V_T(X) F_R(X) \end{aligned}\right\} \tag{7}$$

where

$$\begin{aligned} C_3 &= 10^{-3} \text{ (SI units)} \\ &= 1.515 \times 10^{4} \text{ (U.S. customary units)} \end{aligned}$$

The average power loss over one mesh cycle is obtained by integrating $P_S(X)$ and $P_R(X)$ over the path of contact and then dividing by the length of the path of contact. Since the functions $P_S(X)$ and $P_R(X)$ do not lend themselves to a closed-form analytical solution, a Simpson's rule numerical integration technique is applied. Figure 1, mesh 2, illustrates the implementation of the power loss integration. To obtain the total power lost during the mesh 2 cycle, we must include not only the losses incurred in mesh 2 but also the losses in mesh 1 from point X_3 to X_4 and the losses in mesh 3 from point X_1 to X_2, since the load is being shared by the teeth just entering and leaving engagement during these periods of time. Therefore

$$\overline{P}_S + \overline{P}_R = \frac{1}{X_4 - X_1} \left\{ 2 \int_{X_1}^{X_2} [P_S(X) + P_R(X)]\, dX \right.$$

$$\left. + \int_{X_2}^{X_3} [P_S(X) + P_R(X)]\, dX + 2 \int_{X_3}^{X_4} [P_S(X) + P_R(X)]\, dX \right\} \tag{8}$$

In the numerical integration of these expressions, the sections of the path of contact between X_1 and X_2 and between X_3 and X_4 are each divided into 200 equal steps. The path of contact between X_2 and X_3 is divided into 40 equal steps. Calculation of the average power loss at various step sizes produces convergence of the solution even with very few steps. Thus the use of the step size indicated yields an accurate integration of the functions.

Windage Losses

Gear windage is generally a smaller portion of the overall gear-system loss at low to moderate speeds than at high speeds. (Windage is defined here to be the power required to rotate the pinion and gear in the air-oil atmosphere present within the gearbox. It does not include churning losses, since the gears are assumed not to come in contact with an oil reservoir, nor does it include oil fling-off losses.) Windage increases rapidly with speed. From work done on turbine rotor wheels of references 13 and 14 (see appendix C), the following expression for windage power loss can be written:

$$P_W = C_4\left(1 + 2.3\frac{t}{R}\right)\rho^{0.8} n^{2.8} R^{4.6} \mu^{0.2} \tag{9}$$

where

$$C_4 = 2.04\times10^{-8} \text{ (SI units)}$$
$$= 2.70\times10^{-13} \text{ (U.S. customary units)}$$

The environment within a gearbox is that of an air-oil mixture. Thus the density and viscosity in equation (9) must represent this mixture. In reference 15, an equivalent air-oil mixture density is calculated to simulate a typical environment within a helicopter gearbox, an environment similar to that in most jet-lubricated gearboxes. The equivalent density is calculated for a mixture having a nominal composition of 34.25 parts air to 1 part oil (an oil/air ratio of about 3 percent). For this analysis, both the density and the viscosity are calculated to represent this mixture. Thus

$$\left.\begin{aligned} \rho_{eq} &= \frac{(1)\rho + (34.25)\rho_{air}}{35.25} \\ \mu_{eq} &= \frac{(1)\mu + (34.25)\mu_{air}}{35.25} \end{aligned}\right\} \tag{10}$$

For this analysis, all properties in equation (10) except oil viscosity are assumed constant. Air density and viscosity at 339 K (150° F) are assumed to be

$$\rho_{air} = 1.042 \text{ kg/m}^3 \text{ (0.065 lbm/ft}^3\text{)}$$

$$\mu_{air} = 2\times10^{-5} \text{ N sec/m}^2 \text{ (2.94}\times10^{-9} \text{ lbf sec/in}^2\text{)}$$

Assuming a specific gravity of 0.9 for the oil yields

$$\rho = 899.3 \text{ kg/m}^3 \ (56.2 \text{ lbm/ft}^3)$$

Use of these values results in

$$\left.\begin{aligned} \rho_{eq} &= 26.52 \text{ kg/m}^3 \ (1.66 \text{ lbm/ft}^3) \\ \mu_{eq} &= 0.028\,\mu + C_5 \end{aligned}\right\} \tag{11}$$

where

$$\begin{aligned} C_5 &= 0.019 \text{ (SI units)} \\ &= 2.86\times10^{-9} \text{ (U.S. customary units)} \end{aligned}$$

Combining equation (11) with equation (9) and using gear notation give the windage power loss for the pinion and gear:

$$\left.\begin{aligned} P_{W,g} &= C_6\left(1 + 2.3\frac{\mathscr{F}}{R_g}\right)\left(\frac{n_p}{m_g}\right)^{2.8} R_g^{4.6}(0.028\,\mu + C_5)^{0.2} \\ P_{W,p} &= C_6\left(1 + 2.3\frac{\mathscr{F}}{R_p}\right) n_p^{2.8} R_p^{4.6}(0.028\,\mu + C_5)^{0.2} \end{aligned}\right\} \tag{12}$$

where

$$\begin{aligned} C_6 &= 2.82\times10^{-7} \text{ (SI units)} \\ &= 4.05\times10^{-13} \text{ (U.S. customary units)} \end{aligned}$$

Rolling-Element Support-Bearing Losses

Bearing power loss is a much investigated and diverse subject in itself. However, in this investigation, we are interested in obtaining an engineering estimate of the bearing power loss without the need to resort to a full computer analysis. Accordingly the simple method described by Harris (ref. 9) is used. Of course, other methods or data could be used if available. It is assumed here that the pinion and gear are straddle mounted and centered on the shaft with identical-size deep-groove ball bearings. Furthermore the pitch diameter is assumed to be the arithmetic average of the bearing bore diameter and the outside diameter. These dimensions can be readily found in a bearing catalog along with the bearing static capacity. From reference 9, the friction torque for one bearing is made up of a load-dependent term and a viscous term:

$$M = M_L + M_V \tag{13}$$

The load-dependent term M_L is

$$M_L = z\left(\frac{F_{ST}}{C_s}\right)^y F_\beta D_m \tag{14}$$

For a deep-groove bearing, $z = 0.0009$ and $y = 0.55$. In the case of equally spaced, straddle-mounted spur gears, no significant axial forces are developed, so that $F_\beta = F_{ST}$, and equation (14) becomes

$$M_L = 0.0009 \frac{F_{ST}^{1.55}}{C_s^{0.55}} D_m \tag{15}$$

The viscous term M_V is given as,

for $\nu n > 2000$ (SI units) (0.0215 (U.S. customary units)),

$$M_V = 1.42\times10^{-5} f_o (\nu n)^{2/3} D_m^3 C_7 \tag{16a}$$

for $\nu n \leq 2000$ (SI units) (0.0215 (U.S. customary units)),

$$M_V = 3.492\times10^{-3} f_o D_m^3 C_8 \tag{16b}$$

where

C_7 = 6894 (SI units)

= 2051 (U.S. customary units)

C_8 = 6894 (SI units)

= 1.0 (U.S. customary units)

and f_o is a term used to represent the amount of lubricant in the contact. An f_o value of 2 is selected; it corresponds to that for a partially flooded contact, such as an oil bath or jet-lubricated bearing, an arrangement halfway between a mist and flooded oil lubrication. The torque loss is calculated for both the pinion and the gear bearings and doubled, since there are two bearings on each shaft. The torque loss is then converted to a power loss by multiplying by the appropriate bearing speed:

$$P_{BRG} = 2C_9(M_g n_g + M_p n_p) \tag{17}$$

where

$$C_9 = 1.05\times10^{-4} \text{ (SI units)}$$
$$= 1.59\times10^{-5} \text{ (U.S. customary units)}$$

RESULTS AND DISCUSSION

Simplified Equations for Sliding and Rolling Power Loss

Figure 2 shows the calculated variations of sliding and rolling power loss along the path of contact for the gearset of reference 6 at the full-power test point. It must be noted that the losses include contributions from two sets of teeth when the transmitted load is shared. The simple shapes of these functions suggest that algebraic expressions can be developed to accomplish the integration, so that the equations for sliding and rolling loss are simplified. These simplified expressions are

$$\hat{P}_S = \frac{[P_S(\ell_1) + P_S(\ell_2)]\ell_3 + \dfrac{[P_S(\ell_4)](\ell_5)}{2}}{\ell_6} \tag{18}$$

$$\hat{P}_R = \frac{[P_R(\ell_1) + P_R(\ell_2)]\ell_3 + [P_R(X_P)]\ell_5}{\ell_6} \tag{19}$$

The results from the simplified equations are within 1 percent of the numerically integrated results for a large number of cases.

Comparison of Analysis with Data

The accuracy of the present analysis was validated by comparisons with experimental spur-gear performance data. Part-load gear efficiency data are very limited largely because of the difficultly in accurately measuring small power losses. In the study of reference 6, power loss was measured by the square-loop test method with speed, load, oil viscosity, gear width, location of oil jet, and lubricant flow rate as test variables. Although the present analysis does not account for oil flow rate or jet location, the effects of speed, load, and face width are included and were compared with test data. The support-bearing loss was also measured in the study of reference 6, so

that the gear power loss could be separated from the bearing loss. The gear geometry and operating conditions used in this comparison are listed in table I.

The appropriate oil viscosity to be used in the calculations requires an estimate of the bulk gear tooth temperature at the surface, since calculations of the sliding friction coefficient and the EHD film thickness are based on this temperature. Unfortunately the bulk gear tooth surface temperature is rarely known, so that an estimate must be made. A reasonable approximation can be made by assuming that the bulk tooth surface temperature (not the same as the instantaneous tooth temperature along the path of contact) is equal to the temperature of the oil exiting from the mesh. In the tests of reference 6, only the oil supply temperature of 333 K (140° F) was given. This temperature was used to make an initial estimate of the mesh power loss. The initial calculations indicated that the maximum gear losses are approximately 0.37 kilowatt (0.5 hp). If the entire 0.37 kilowatt (0.5 hp) were transmitted to the oil at the lowest flow rate tested, 1.9 liters per minute (0.5 gal/min), the maximum mesh exit oil temperature would be 340 K (153° F). Therefore, a nominal bulk gear surface temperature of 339 K (150° F) was selected, and the approximate absolute oil viscosity to be used in the gear power loss calculations was then 0.05 N sec/m^2. Since the temperature rise across the bearing is small, the calculations of bearing power loss use the absolute viscosity at the supply oil jet temperature of 333 K (140° F), 0.054 N sec/m^2. An example calculation for the maximum-power test point of reference 6 is given in table III.

In figure 4 the calculated gear losses (excluding bearing losses) are compared with the test data of reference 6 for a gear width of 0.04 meter (1.563 in.) and for various lubricant flow rates, oil jet positions, and pinion speeds as a function of pinion torque. Also shown is the gear power loss as calculated by the method of reference 5. Oil flow rate was held at either 1.9 or 11.4 liters per minute (0.5 or 3 gal/min), and the oil supply jet was positioned so that the oil impinged on either the inlet or the outlet side of the mesh. In all cases, the measured power loss was greatest at the higher flow rate with the oil jet positioned at the inlet to the mesh. The current analysis predicts slightly higher power losses than measured, but predicts with reasonable accuracy the sensitivity of gear mesh power loss to speed and load. The analysis of reference 5 predicted significantly greater power loss than the current analysis. The reason for the difference between the current analysis and the prediction from reference 5 lies, principally, in the friction-coefficient expressions used. In figure 4 as speed is increased, the power loss becomes more sensitive to changes in the applied loads. This change in sensitivity can be understood if the power loss is considered as a loss of torque at the drive pinion shaft. At each operating speed, there is some variation in torque loss as a function of load, but the variation is small. The power loss is the product of torque loss and pinion speed. The pinion speed amplifies the torque loss when expressed as power. Most of the change in sensitivity of power loss with speed shown in figure 4 is due to amplification of the torque loss by the operating speed.

In figure 5, the measured bearing losses of reference 6 are compared with predicted results. The calculated bearing losses are approximately 25 percent low at each speed, but the load sensitivity is accurate.

In figure 6, the gear and bearing losses are combined and shown as overall gearbox efficiency as a function of pinion torque. The calculated efficiency is within 0.3 percentage point of the measured results at an oil flow rate of 11.4 liters per minute (3 gal/min) with oil supplied into the mesh. When the analytical results are compared with the experimental data for the other lubricant flow rates and oil jet positions, the largest difference occurs at low torque and high speed with the most efficient lubrication method, namely, a flow rate of 1.9 liters per minute (0.5 gal/min) and the oil supplied to the exit of the mesh. At this condition, the analysis predicts an efficiency that is 0.6 percentage point lower than the measured value. The predicted trends with speed and torque generally show good agreement with the data.

In the tests of reference 6, data were also taken on a gear of larger face width but of the same basic geometry (see table I). Figure 7 shows the predicted system efficiency for the wider gear. The part-load efficiency for this gear drops more substantially at higher speeds than the narrower gear. The analysis correctly predicts this lower efficiency. As in the previous case, the calculated values agree closely with the test data for the least efficient method of lubrication. The test data at 250 rpm for the wider gear show more variation between the types of lubrication. For this geometry, the greatest deviation between the analytical and measured data is 0.7 percentage point, at 2000 rpm and 67.8-newton-meter (50-ft-lbf) pinion torque. When the analysis is compared with the data for 11.4 liters per minute (3 gal/min), the maximum difference is 0.5 percentage point at 250 rpm and 67.8 newton-meters (50 ft-lbf). Once again the analysis shows remarkably good agreement in speed and load variation with the test data.

In the event that full-load gear-system data become available either empirically or through another analytical technique, the present analysis could be calibrated to match these data at the full-load efficiency point. The adjusted analysis could then be used with a high degree of confidence to predict off-speed and off-load design-point performance.

Breakdown of Gear-System Losses

With the gear loss prediction method presented in this study, the theoretical contributions of the individual component losses to the total gear mesh loss can be readily determined at any speed and applied load. An example of this is given in figure 8, which shows a theoretical percentage breakdown of the various components of gear-system power loss for the 0.04-meter-(1.563-in.-) wide test gear as a function of applied load

for three speeds. At low speeds, the sliding loss accounts for most of the system loss. At higher speeds, the sliding loss becomes less important, and the rolling loss and the pinion bearing losses become significant. Gear and pinion windage are often neglected. At low speeds, this is justified. However, at higher speeds such as the value 2000 rpm used in this example, windage contributes as much as 10 percent of the total power loss and should not be neglected. At low torque, the sliding loss is low, since this loss is a direct function of load. The rolling loss is proportional to film thickness, which is relatively insensitive to load. Therefore rolling loss dominates at low torque.

Figure 8(c) shows the error in using the sliding loss alone, that is, using just a gear coefficient of friction, to predict gear efficiency as suggested by several investigators (refs. 1 to 3). At the full load of 271 newton-meters (200 ft-lbf), the sliding component represents only about one-half of the gear losses, excluding bearing losses. The rolling and windage losses account for the other 50 percent and must be properly accounted for to obtain an accurate estimate of gear power loss. In addition, figure 8 clearly shows that using the coefficient of friction to predict part-load gear efficiency is grossly inadequate, since the sliding power loss decreases to zero at low loads.

Finally, figure 8 illustrates the fact that the rolling-element support-bearing losses are generally a significant portion of the total system losses and should not be ignored. In the case of the test gears that were analyzed, the bearing power loss varied from about 10 percent of the total system power loss at the lowest speed and highest torque to about 40 percent of the total at the highest speed and zero load.

Figure 9 shows the power loss of the spur-gear system described in reference 6 as a percentage of the full-load power loss at several levels of loading. The lowest loading curve (an input torque of 0.54 N-m (0.4 ft-lbf)) represents the no-load or tare-loss curve. It is instructive to note that the tare power loss of an unloaded gearset theoretically can reach 65 percent of the full-load loss (at an input torque of 271 N-m (200 ft-lbf) and a speed of 2000 rpm). This effect is due to the fact that at higher speeds the rolling, windage, and support-bearing losses are relatively insensitive to load but make up a major part of the system loss. As the load is decreased, only the load-dependent sliding loss decreases, and the system loss remains high.

SUMMARY OF RESULTS

A simple method for predicting the power loss and efficiency of a steel spur gearset of arbitrary geometry supported by ball bearings was developed. The method algebraically accounts for losses due to gear sliding, rolling, and windage and incorporates an expression for ball-bearing power loss. This method provides an accurate estimate of spur-gear-system efficiency at part load as well as full load. The analysis was compared with test data generated on a recirculating-power spur-gear test rig from another

investigation for a wide range of speeds and loads and for various methods of gear lubrication. The theoretical contributions of the individual component losses were compared with the total gear-system loss. The following results were obtained:

1. The analysis generally showed good agreement with the test data at all conditions except low oil flow rates, where the analysis slightly underestimated the measured gear-system efficiency.

2. The predicted sensitivity of power loss to change in speed and load closely resembled that determined experimentally.

3. The contributions of gear rolling-traction loss and support-bearing loss to the total system loss were significant. The contribution of windage was also significant, but to a lesser degree. These losses should be accounted for in the loss calculation, particularly under part-load conditions.

4. The unloaded or tare power loss of the gear system at operating speed could be as much as 65 percent of the maximum-load loss.

Lewis Research Center,
National Aeronautics and Space Administration,
Cleveland, Ohio, December 10, 1979,
505-04.

APPENDIX A

EQUATIONS USED IN CALCULATIONS OF GEAR POWER LOSS

Equations for Path of Contact

The path of contact is a line in space mapped out by the point of contact of two gears in mesh. The path of contact is a straight line for involute gear geometry. The points X_1 to X_4 shown in figure 1 and X_P represent the following sequence of events:

(1) X_1 - start of mesh cycle, two teeth share the load
(2) X_2 - start of single-tooth contact
(3) X_3 - end of single-tooth contact
(4) X_4 - end of mesh cycle
(5) X_P - pitch point

The following equations for these points are given in reference 3:

$$D_g = \frac{C_{10} N_g}{\mathscr{P}}$$

$$D_p = \frac{C_{10} N_p}{\mathscr{P}}$$

$$D_{o,p} = D_p \cos\theta$$

$$D_{a,p} = D_p + \frac{2C_{10}}{\mathscr{P}}$$

$$D_{o,g} = D_g \cos\theta$$

$$D_{a,g} = D_g + \frac{2C_{10}}{\mathscr{P}}$$

$$\mathscr{P}_b = \frac{D_{o,p}\pi}{N_p}$$

$$X_A = \frac{(D_p + D_g)\sin\theta}{2}$$

(A1)

(continued)

$$
\left.
\begin{aligned}
X_1 &= X_A - 0.5\left(D_{a,g}^2 - D_{o,g}^2\right)^{1/2} \\
X_3 &= X_1 + \not{p}_b \\
X_4 &= 0.5\left(D_{a,p}^2 - D_{o,p}^2\right)^{1/2} \\
X_2 &= X_4 - \not{p}_b \\
X_P &= X_1 + C_{10}\left[\left(\frac{2 + N_p m_g}{2\not{p}}\right)^2 - \left(\frac{N_p m_g \cos\theta}{2\not{p}}\right)^2\right]^{1/2} - \frac{C_{10} N_p m_g \sin\theta}{2\not{p}}
\end{aligned}
\right\} \quad \text{(A1)}
$$

where

$$
\begin{aligned}
C_{10} &= 0.0254 \text{ (SI units)} \\
&= 1.0 \text{ (U.S. customary units)}
\end{aligned}
$$

Six additional lengths along the path of contact are required in the sliding and rolling power loss calculations:

$$
\left.
\begin{aligned}
\ell_1 &= \frac{X_1 + X_2}{2} \\
\ell_2 &= \ell_1 - X_1 + X_3 \\
\ell_3 &= X_4 - X_3 + X_2 - X_1 \\
\ell_4 &= X_2 + \Delta\ell \\
\ell_5 &= X_3 - X_2 \\
\ell_6 &= X_4 - X_1
\end{aligned}
\right\} \quad \text{(A2)}
$$

where

$$
\Delta\ell = 3\times10^{-5}\text{m}(0.001 \text{ in.})
$$

Sliding and Rolling Velocity

The sliding velocity is the difference in surface velocity of the two gears at the point of contact. The sliding velocity varies along the path of contact and changes direction at the pitch point. Since we are interested only in the magnitude of the sliding velocity, we eliminate the change of sign by taking the absolute value of $X - X_P$:

$$V_S(X) = V_g - V_p = (\omega_g + \omega_p)|X - X_P| \tag{A3}$$

or in terms of pinion speed

$$V_S(X) = \frac{0.1047(1 + m_g)n_p|X - X_P|}{m_g} \tag{A4}$$

The rolling velocity as defined in the Benedict and Kelley friction coefficient (ref. 8) is

$$V_T = V_g + V_p$$

In reference 5, the rolling velocity is shown to be

$$V_T = V_g + V_p = 2V\frac{\sin\theta - |X - X_P|(m_g - 1)}{m_g D_p}$$

This equation can be rewritten in terms of pinion speed as

$$V_T(X) = 0.1047\, n_p D_p \frac{\sin\theta - |X - X_P|(m_g - 1)}{D_g} \tag{A5}$$

Gear Load

The normal load on the gear tooth surface may be calculated from the applied pinion torque:

$$\left.\begin{aligned} w_T &= \frac{T_p}{\frac{D_p}{2}} \\ w_n &= \frac{w_T}{\cos\theta} \\ w_n &= \frac{2T_p}{D_p \cos\theta} \end{aligned}\right\} \tag{A6}$$

Between points X_2 and X_3 along the path of contact, w_n is carried by one tooth. Between X_1 and X_2 and between X_3 and X_4, the load is shared by two gears. Thus

$$\left.\begin{aligned} w(X) &= w_n \quad \text{for } X_2 \le X \le X_3 \\ w(X) &= \frac{w_n}{2} \quad \text{for } X_1 < X < X_2 \\ &\qquad \text{and } X_3 < X < X_4 \end{aligned}\right\} \tag{A7}$$

Equivalent Rolling Radius

The gear contact can be approximated by two equivalent rollers in contact. The equivalent roller radius changes along the path of contact and can be found as follows:

$$\left.\begin{aligned} R_{o,g} &= \frac{D_p \sin\theta}{2} + |X - X_p| \\ R_{o,p} &= \frac{D_g \sin\theta}{2} - |X - X_p| \\ R_{eq} &= \frac{R_{o,g} R_{o,p}}{R_{o,g} + R_{o,p}} \end{aligned}\right\} \tag{A8}$$

APPENDIX B

FILM-THICKNESS EQUATION FOR CALCULATION OF ROLLING POWER LOSS

Adaptation of Film Thickness Equation of Reference 11 to Gear Geometry

The expression for central film thickness in an EHD contact developed in reference 11 is

$$H_H = 2.69\, R_x U^{0.67} G^{0.53} W^{-0.067} (1 - 0.61\, e^{-0.73k}) \qquad \text{(B1)}$$

This general EHD equation is modified here to incorporate gear parameters by taking each nondimensional grouping and explaining its application to the gear contact:

U speed parameter, $u\mu_0/E'R_x$

u surface velocity; in a gear contact, the average rolling velocity is used for u; since V_T is defined as $V_g + V_p$ here, $u = V_T/2$

μ_0 atmospheric absolute viscosity of lubricant, N sec/m^2 (lbf sec/in^2)

E' $2\Big/\left(\dfrac{1-\gamma_g^2}{E_g} + \dfrac{1-\gamma_p^2}{E_p}\right)$; if we assume that both the gear and the pinion are made of steel, $E' = 2.276\times10^{11}$ N/m^2 (33×10^6 lbf/in^2)

R_x equivalent rolling radius as defined in equation (A8), $R_{eq}(X)$

G material parameter, $E'\alpha$, 4617

α pressure-viscosity coefficient; for a typical mineral-oil gear lubricant, 2.030×10^{-8} m^2/N (1.4×10^{-4} in^2/lbf)

W load parameter, $F_H/E'R_x^2$

F_H normal load on EHD contact; in gear contact, $F_H = w(X)$, as defined in appendix A (under Gear Load)

k elliplicity parameter, a/b; a and b define size of contact area; for gears in line contact, a constant value of 12 is assumed

Combining these constants and variables gives

$$h(X) = C_{11}[V_T(X)\mu_0]^{0.67}[w(X)]^{-0.067}[R_{eq}(X)]^{0.464} \qquad \text{(B2)}$$

where

$$C_{11} = 2.051\times10^{-7} \text{ (SI units)}$$
$$= 4.34\times10^{-3} \text{ (U.S. customary units)}$$

Thermal Reduction Factor

At high pitch line velocities, the film thickness calculated by equation (B2) overestimates the actual film thickness. In reference 12, a thermal reduction factor is developed to correct for the inlet oil shear heating that occurs in high-speed EHD contacts. The thermal reduction factor φ_t is reproduced in figure 3 as a function of Q_m. The value of Q_m can be calculated as follows:

$$Q_m(X) = \frac{C_{12}\mu_0 u^2 \delta}{K_f} \tag{B3}$$

where

$$C_{12} = 1\times10^{-3} \text{ (SI units)}$$
$$= 4.629 \text{ (U.S. customary units)}$$

Since u is defined as the average surface velocity in reference 12, we must use $u = V_T(X)/2$. The thermal conductivity of the lubricant K_f is assumed to be constant. A typical value of K_f for a mineral-oil lubricant is

$$K_f = 0.125 \text{ W/m K } (0.0725 \text{ Btu/hr ft } ^oF)$$

If the viscosity-temperature characteristics are known, δ can be found for a given oil. The following equation must be solved for δ by using known values of μ at temperature β and of μ_0 at temperature β_0:

$$\mu = \mu_0 e^{[-\delta(\beta-\beta_0)+\alpha p]}$$

At atmospheric pressure, $p = 0$; thus

$$\delta = \frac{\ln \mu_0 - \ln \mu}{\beta - \beta_0}$$

For a typical mineral-oil lubricant,

$$\delta = 0.034\ K^{-1}(0.019\ ^{o}F^{-1})$$

Combining these values in equation (B3) yields

$$Q_m = C_{13}\mu_0[V_T(X)]^2 \tag{B4}$$

where

$$C_{13} = 6.8\times10^{-5}\ \text{(SI units)}$$
$$= 0.303\times10^{-8}\ \text{(U.S. customary units)}$$

After Q_m has been calculated, φ_t can be found in figure 3.

APPENDIX C

WINDAGE POWER LOSS EQUATION

An expression for gear windage loss is developed here from data obtained in the studies of references 13 and 14 on turbine rotor windage losses. The moment coefficient for a rotating disk is commonly expressed as

$$C_m = \frac{C_{14}T}{\frac{1}{2}\rho\omega^2 R^5} \tag{C1}$$

where

$$C_{14} = 1.0 \text{ (SI units)}$$
$$= 1.5\times10^{-6} \text{ (U.S. customary units)}$$

This coefficient was evaluated experimentally and found to be of the form

$$C_m = \frac{K}{Re^{\epsilon}} \tag{C2}$$

(refs. 13 and 14). This expression was modified to account for disk width as follows:

$$C_m = C_{m,0}\left(1 + 2.3\,\frac{t}{R}\right) \tag{C3}$$

where $C_{m,0}$ is the moment coefficient for a disk of zero thickness (ref. 13). This equation was verified for ratios of disk thickness to radius up to 0.15.

Reference 13 gives equation (C2) as

$$C_{m,0} = \frac{0.09}{Re^{0.21}} \tag{C4}$$

for the unbladed disk. Reference 14 gives equation (C2) as

$$C_{m,0} = \frac{0.102\left(\frac{S}{R}\right)^{0.1}}{Re^{0.20}} \tag{C5}$$

where S is the axial clearance between the rotor and the housing wall, and R is the radius of the disk. (In ref. 14, the constant 0.102 is printed as 0.0102 in the expression for C_m. Inspection of the data indicates that this constant must be 0.102.) Equation (C5) applies when turbulent flow exists within the gearbox and the wall and gear boundary layers are not merged.

In a gearbox application, generally there is significant axial clearance between the gear and the housing wall. For this analysis, S/R = 0.217 (the largest value in ref. 14) is used. Thus equation (C5) becomes

$$C_{m,0} = \frac{0.0876}{Re^{0.20}} \tag{C6}$$

This value agrees with equation (C4) from reference 13. Combining equations (C1), (C3), and (C6) results in

$$C_m = \frac{C_{14}T}{\frac{1}{2}\rho\omega^2R^5} = \left(1 + 2.3\,\frac{t}{R}\right)\frac{0.09}{Re^{0.2}} \tag{C7}$$

The drag torque T is

$$T = \frac{C_{14}\rho\omega^2R^5}{2}\left(1 + 2.3\,\frac{t}{R}\right)\frac{0.09}{Re^{0.2}}$$

Converting this equation to a power loss and simplifying yield

$$\mathcal{P}_W = C_4\left(1 + 2.3\,\frac{t}{R}\right)\rho^{0.8}n^{2.8}R^{4.6}\mu^{0.2} \tag{C8}$$

where

$$C_4 = 2.04\times10^{-8} \text{ (SI units)}$$
$$= 2.70\times10^{-13} \text{ (U.S. customary units)}$$

REFERENCES

1. Shipley, Eugene E.: Loaded Gears in Action. Gear Handbook, D. W. Dudley, ed., McGraw Hill Book Co., Inc., 1962, ch. 14, pp. 14-1-14-60.

2. Buckingham, Earle: Efficiencies of Gears. Analytical Mechanics of Gears, Dover Publications, Inc., 1963, ch. 19, pp. 395-425.

3. Merritt, H. E.: Efficiency and Testing. Gear Engineering, John Wiley and Sons, Inc., 1972, ch. 22, pp. 345-357.

4. Martin, K. F.: A Review of Friction Predictions in Gear Teeth. Wear, vol. 49, no. 2, Aug. 1978, pp. 201-238.

5. Chiu, Y. P.: Approximate Calculation of Power Loss in Involute Gears. ASME Paper 75-PTG-2, Oct. 1975.

6. Fletcher, H. A. G.; and Bamborough, J.: Effect of Oil Viscosity and Supply Conditions on Efficiency of Spur Gearing. NEL-138, National Engineering Laboratory, Glasgow, 1964.

7. Cameron, A.: Rolling Contacts, Discs and Spheres. Principles of Lubrication, John Wiley and Sons, Inc., 1966, ch. 7, pp. 154-185.

8. Benedict, G. H.; and Kelley, B. W.: Instantaneous Coefficients of Gear Tooth Friction. ASLE Trans., vol. 4, no. 1, Apr., 1961, pp. 59-70.

9. Harris, T. A.: Rolling Bearing Analysis. John Wiley and Sons, Inc., 1966.

10. Crook, A. W.: The Lubrication of Rollers. IV. Measurements of Friction and Effective Viscosity. Phil. Trans. Roy. Soc. (London), ser. A., vol. 255, no. 1056, Jan. 17, 1963, pp. 281-312.

11. Hamrock, B. J.; and Dowson, D.: Isothermal Elastohydrodynamic Lubrication of Point Contacts. III - Fully Flooded Results. J. Lub. Tech., vol. 99, no. 2, Apr. 1977, pp. 264-276.

12. Cheng, H. S.: Prediction of Film Thickness and Traction in Elastohydrodynamic Contacts. ASME Design Engineering Technology Conference, American Society of Mechanical Engineers, New York, N. Y., 1974, pp. 285-293.

13. Mann, R. W.; and Marston, C. H.: Friction Drag on Bladed Discs in Housings. J. Basic Eng., vol. 83, no. 4, Dec. 1961, pp. 719-723.

14. Daily, J. W.; and Nece, R. E.: Chamber Dimension Effects on Induced Flow and Frictional Resistance of Enclosed Rotating Disks. J. Basic Eng., vol. 82, no. 1, Mar. 1960, pp. 217-232.

15. Bowen, C. W.; Braddock, C. E.; and Walker, R. D.: Installation of a High-Reduction-Ratio Transmission in the UH-1 Helicopter. USAAVLABS-TR-68-57, U.S. Army Aviation Materiel Laboratories, 1969. (AD-855747.)

TABLE I. - GEAR GEOMETRY AND OPERATING PARAMETERS

FOR TEST GEARS OF REFERENCE 6

Pitch diameter, cm (in.)	
Pinion	15.2(6)
Gear	25.4(10)
Number of teeth	
Pinion	48
Gear	80
Diametral pitch	8
Pressure angle, deg	20
Width, cm (in.)	4.0(1.563) or 7.94(3.125)
Lubricant	Mineral oil with antioxidant additive
Viscosity at oil jet temperature of 333 K (140° F), cm^2/sec	0.60

TABLE II. - CONSTANTS USED IN GEAR POWER

LOSS EQUATIONS

Constant	Value for SI units	Value for U.S. customary units
C_1	29.66	45.94
C_2	9.0×10^{7}	1.3×10^{4}
C_3	1×10^{-3}	1.515×10^{-4}
C_4	2.04×10^{-8}	2.70×10^{-13}
C_5	.019	2.86×10^{-9}
C_6	2.82×10^{-7}	4.05×10^{-13}
C_7	6894	2051
C_8	6894	1.0
C_9	1.05×10^{-4}	1.59×10^{-5}
C_{10}	.0254	1.0
C_{11}	2.051×10^{-7}	4.34×10^{-3}
C_{12}	1×10^{-3}	4.629
C_{13}	6.8×10^{-5}	.303
C_{14}	1.0	1.5×10^{-6}

TABLE III. - SUMMARY OF POWER LOSS EQUATIONS FOR SPUR-GEAR SYSTEM AND DESIGN EXAMPLE

[Gear data: N_p, 48; N_g, 80; $\mathscr{P}$, 8; θ, 20°; m_g, 1.666; $\mathscr{F}$, 0.0397 m (1.5625 in.); operating conditions: n_p, 2000 rpm; T_p, 271 N-m (2400 in.-lbf); μ_0, 0.05 N sec/m^2 (7.25×10^{-6} lbf sec/in^2); ν_B, 0.60 cm^2/sec (6.459×10^{-4} ft^2/sec); f_o, 2; bearing data: D_m, 0.07 m (2.75 in.); C_s, 17 436 N (3920 lbf); F_{ST} = w.]

(a) Equations for path of contact, windage loss, and bearing loss

Parameter	Symbol	Formula	Result
Gear pitch diameter, m (in.)	D_g	$C_{10}N_g/\mathscr{P}$	0.2540(10.00)
Pinion pitch diameter, m (in.)	D_p	$C_{10}N_p/\mathscr{P}$	0.1524(6.000)
Pinion base circle diameter, m (in.)	$D_{o,p}$	$D_p \cos\theta$	0.1432(5.638)
Pinion tip diameter, m (in.)	$D_{a,p}$	$D_p + 2C_{10}/\mathscr{P}$	0.1588(6.250)
Gear base circle diameter, m (in.)	$D_{o,g}$	$D_g \cos\theta$	0.2387(9.3969)
Gear tip diameter, m (in.)	$D_{a,g}$	$D_g + 2C_{10}/\mathscr{P}$	0.2604(10.25)
Base pitch, m (in.)	p_b	$D_{o,p}\pi/N_p$	9.372×10^{-3}(0.3690)
Length between interference points, m (in.)	X_A	$(D_p + D_g)\sin\theta/2$	69.50×10^{-3}(2.736)
Start of double-tooth contact, m (in.)	X_1	$X_A - 0.5\left(D_{a,g}^2 - D_{o,g}^2\right)^{1/2}$	17.47×10^{-3}(0.6890)
End of single-tooth contac, m (in.)	X_3	$X_1 + p_b$	26.84×10^{-3}(1.058)
End of mesh cycle, m (in.)	X_4	$0.5\left(D_{a,p}^2 - D_{o,p}^2\right)^{1/2}$	34.32×10^{-3}(1.349)
End of double-tooth contact, m (in.)	X_2	$X_4 - p_b$	24.95×10^{-3}(0.9799)
Pitch point, m (in.)	X_P	$X_1 + C_{10}\left\{[(2 + N_p m_g)/2\mathscr{P}]^2 - (N_p m_g \cos\theta/2\mathscr{P})^2\right\}^{1/2} - C_{10}N_p m_g \sin\theta/2\mathscr{P}$	26.03×10^{-3}(1.026)

Midpoint between X_1 and X_2, m (in.)	ℓ_1	$(X_1 + X_2)/2$	$21.20\times10^{-3}(0.8345)$
Midpoint between X_3 and X_4, m (in.)	ℓ_2	$\ell_1 - X_1 + X_3$	$30.60\times10^{-3}(1.204)$
Length of single-tooth contact, m (in.)	ℓ_3	$X_4 - X_3 + X_2 - X_1$	$14.96\times10^{-3}(0.5818)$
Start of double-tooth contact, m (in.)	ℓ_4	$X_2 + \Delta\ell$	$24.98\times10^{-3}(0.9809)$
Length of double-tooth contact, m (in.)	ℓ_5	$X_3 - X_2$	$18.94\times10^{-3}(0.0744)$
Total length of contact, m (in.)	ℓ_6	$X_4 - X_1$	$16.85\times10^{-3}(0.6599)$
Gear tooth normal load, N(lbf)	w_n	$2T_p/(D_p \cos\theta)$	3785(850.9)
Gear windage loss, kW (hp)	$P_{W,g}$	$C_6(1 + 2.3\mathscr{F}/R_g)(n_p/m_g)^{2.8}R_g^{4.6}(0.028\,\mu_0 + C_5)^{0.2}$	0.0164(0.0220)
Pinion windage loss, kW (hp)	$P_{W,p}$	$C_6(1 + 2.3\mathscr{F}/R_p)n_2^{2.8}R_p^{4.6}(0.028\,\mu_0 + C_5)^{0.2}$	0.0084(0.0112)
Gear bearing load-dependent torque, N-m (in-lb)	$M_{L,g}$	$0.0009\,F_{ST}^{1.55}C_s^{-0.55}D_m$	0.0351(0.3107)
Pinion bearing load-dependent torque, N-m (in-lb)	$M_{L,p}$	$0.0009\,F_{ST}^{1.55}C_s^{-0.55}D_m$	0.0351(0.3107)
Gear bearing viscous torque, N-m (in-lbf)	$M_{V,g}$	$C_7\,1.42\times10^{-5}\,f_o(\nu_B n_g)^{2/3}D_m^3$	0.1079(1.024)
Pinion bearing viscous torque, N-m (in-lbf)	$M_{V,p}$	$C_7\,1.42\times10^{-5}\,f_o(\nu_B n_p)^{2/3}D_m^3$	0.1634(1.437)
Total gear bearing torque loss, N-m (in-lbf)	M_g	$M_{L,g} + M_{V,g}$	0.1430(1.335)
Total pinion bearing torque loss, N-m (in-lbf)	M_p	$M_{L,p} + M_{V,p}$	0.1985(1.748)
Total support-bearing power loss, kW (hp)	P_{BRG}	$2C_9(M_g n_g + M_p n_p)$	0.1194(0.1620)

TABLE III. - Concluded.

(b) Mesh losses along path of contact

Parameter	Symbol	Formula	Result at -			
			$X = \ell_1$	$X = \ell_2$	$X = \ell_4$	$X = X_P$
Sliding velocity, m/sec (in/sec)	V_S	$0.0147(1 + m_g)n_p(X - X_P)/m_g$	1.608(64.17)	1.542(59.48)	0.3418(15.11)	0
Rolling velocity, m/sec (in/sec)	V_T	$0.1047\, n_p D_p[\sin\theta - \lvert X - X_P\rvert(m_g - 1)/D_g]$	10.51(413.7)	10.53(414.9)	10.83(426.2)	10.91(429.7)
Tooth normal load, N (lbf)	w	w_n or $w_n/2$ (a)	(1892)(425.7)	1892(425.7)	3785(851.3)	3785(851.3)
Friction coefficient	f	$0.0127 \log\left[C_1 w/\left(f\mu_0 V_S V_T^2\right)\right]$	0.0279	0.0282	0.0394	----------
Sliding power loss, kW (hp)	P_S	$C_3 V_S f w$	0.0852(0.1155)	0.0823(0.1082)	0.0420(0.0768)	----------
Gear equivalent radius, m (in.)	$R_{o,g}$	$D_p(\sin\theta)/2 + \lvert X - X_P\rvert$	0.0309(1.218)	0.0307(1.204)	0.0271(1.071)	0.0261(1.026)
Pinion equivalent radius, m (in.)	$R_{o,p}$	$D_g(\sin\theta)/2 - \lvert X - X_P\rvert$	0.0386(1.519)	0.0388(1.533)	0.0424(1.665)	0.0434(1.710)
Equivalent contact radius, m (in.)	R_{eq}	$R_{o,g}R_{o,p}/(R_{o,g} + R_{o,p})$	0.0172(0.6758)	0.0172(0.6742)	----------	0.0163(0.6413)
Film thickness, m (in.)	h	$C_{11}(V_T\mu_0)^{0.67}w^{-0.067}R_{eq}^{0.464}$	$1.247\times10^{-6}(49.20\times10^{-6})$	$1.248\times10^{-6}(49.24\times10^{-6})$	----------	$1.192\times10^{-6}(47.02\times10^{-6})$
Thermal loading factor	Q_m	$C_{13}\mu_0 V_T^2$	0.376	0.377	----------	0.405
Thermal reduction factor	φ_t	(b)	0.931	0.931	----------	0.924
Rolling power loss, kW (hp)	P_R	$C_2 C_3 V_T h \varphi_t f$	0.0436(0.0583)	0.0437(0.0585)	----------	0.0429(0.0575)

[a]See fig. 1.

[b]See fig. 3.

(c) Average mesh loss and system efficiency

Parameter	Symbol	Formula	Result
Sliding power loss, kW (hp)	$\hat{P}_S$	$\left\{\left\|P_S(\ell_1) + P_S(\ell_2)\right\|\ell_3 + (P_S(\ell_4))(\ell_5)/2\right\}\Big/\ell_6$	0.1511(0.2016)
Rolling power loss, kW (hp)	$\hat{P}_R$	$\left\{\left\|P_R(\ell_1) + P_R(\ell_2)\right\|\ell_3 + (P_R(X_P))\ell_5\right\}\Big/\ell_6$	0.0823(0.1095)
Total system power loss, kW (hp)	P_{TOT}	$\hat{P}_S + \hat{P}_R + P_{W,g} + P_{W,p} + P_{BRG}$	0.3776(0.5063)
Power into gearset, kW (hp)	P_{IN}	$T_p n_p$	56.79(76.2)
System efficiency, percent	η	$P_{IN} - P_{TOT}/P_{IN} \times 100$	99.34

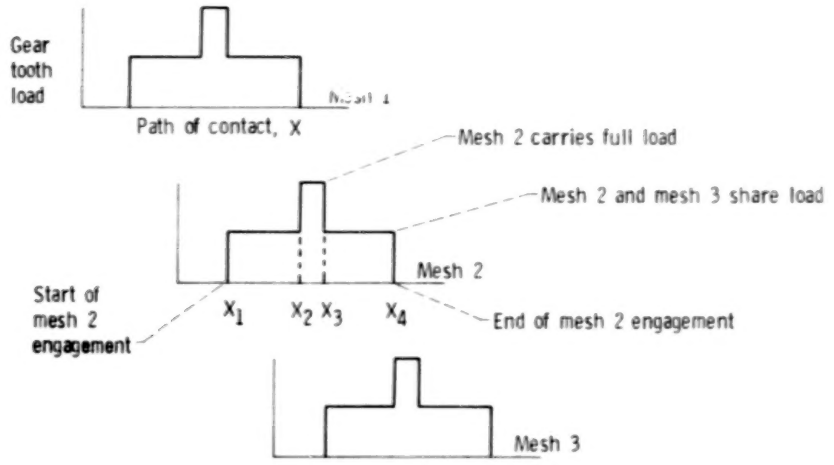

Figure 1. - Tooth load sharing.

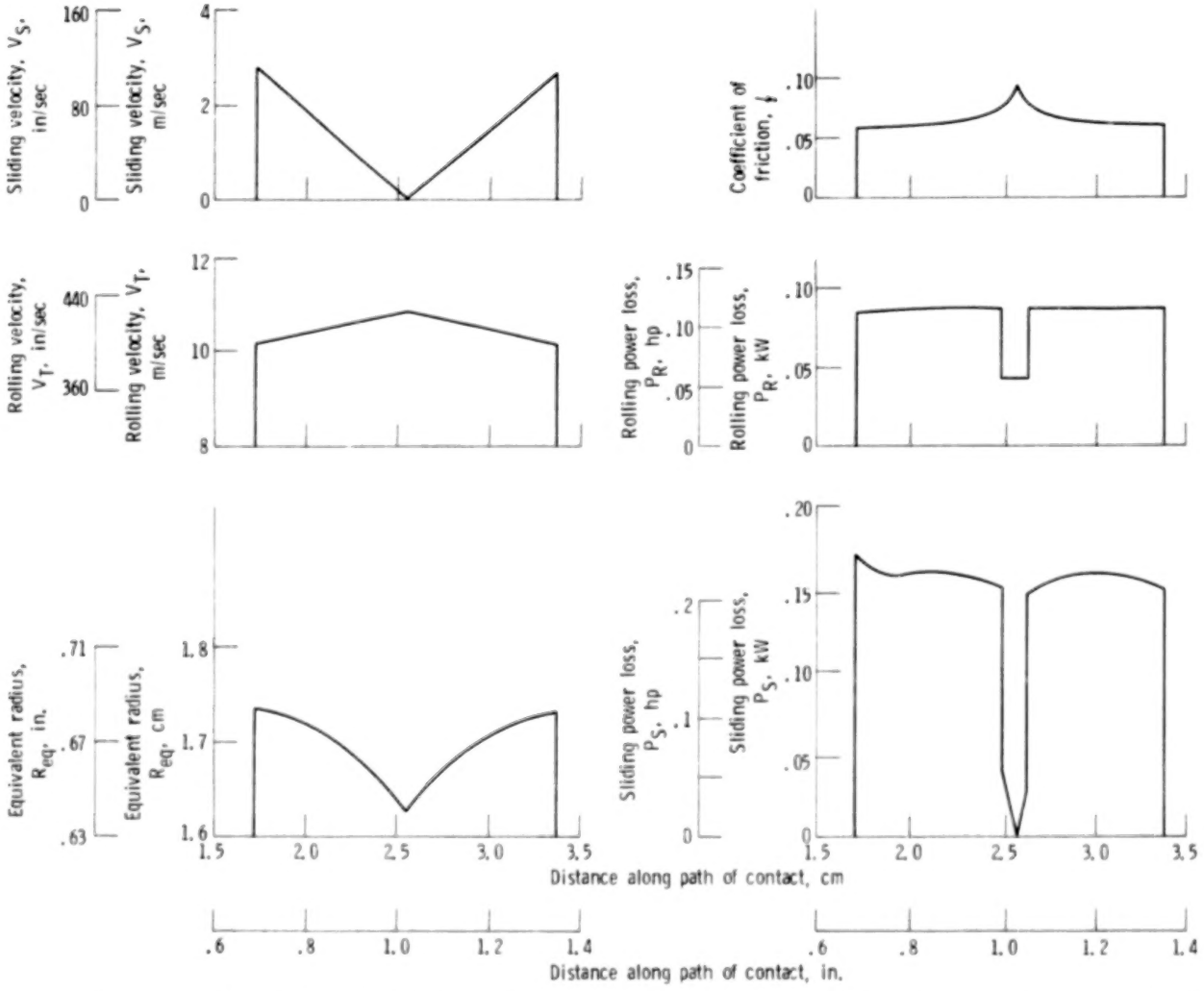

Figure 2. - Instantaneous values of rolling velocity, sliding velocity, coefficient of friction, rolling power loss, and sliding power loss across path of contact of 4.0-centimeter-(1.563-in.-) wide gear of reference 6. Pinion speed, 2000 rpm; pinion torque, 271 newton-meters (200 ft-lb).

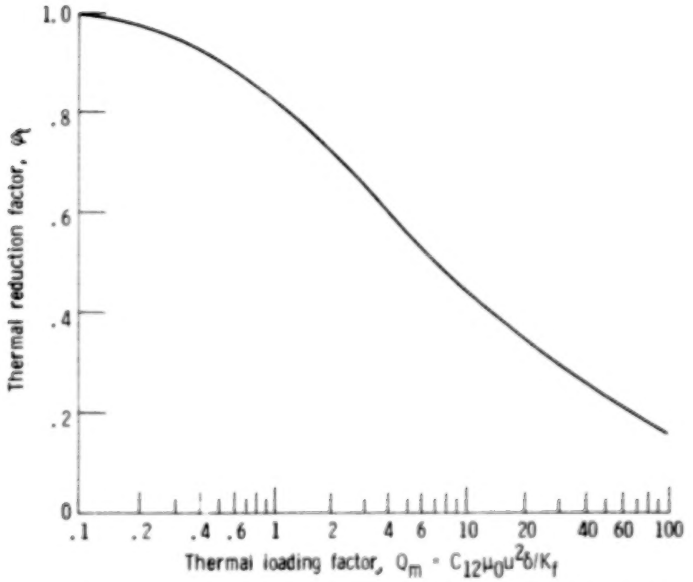

Figure 3. - Film-thickness thermal reduction factor as presented in reference 12.

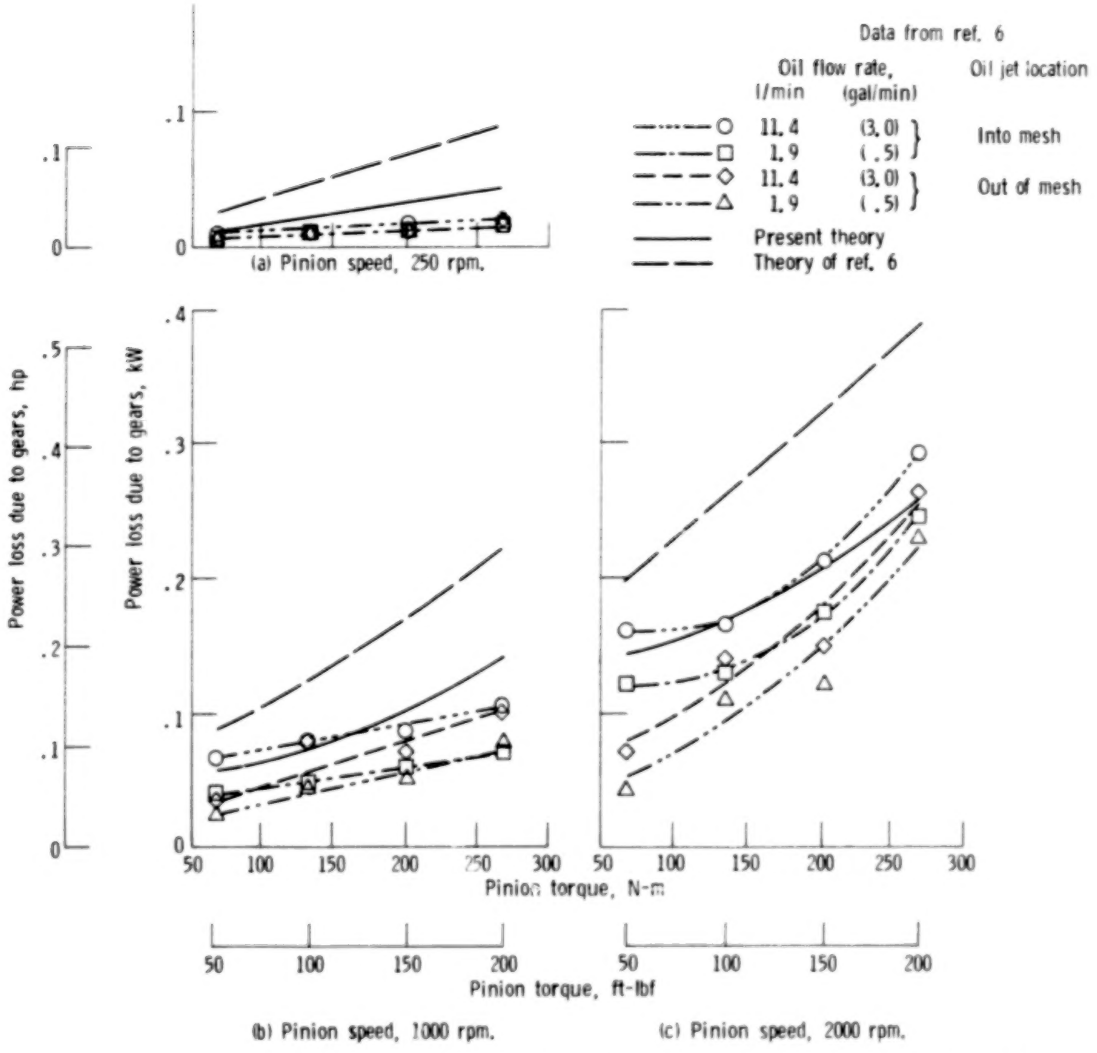

Figure 4. - Comparison of predicted gear power loss with data of reference 6. Gear width, 4.0 centimeters (1.563 in.).

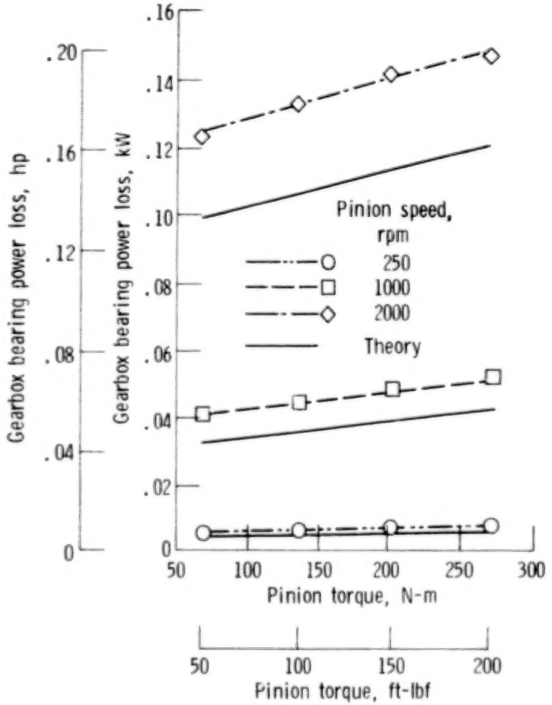

Figure 5. - Comparison of predicted gearbox bearing power loss with data of reference 6.

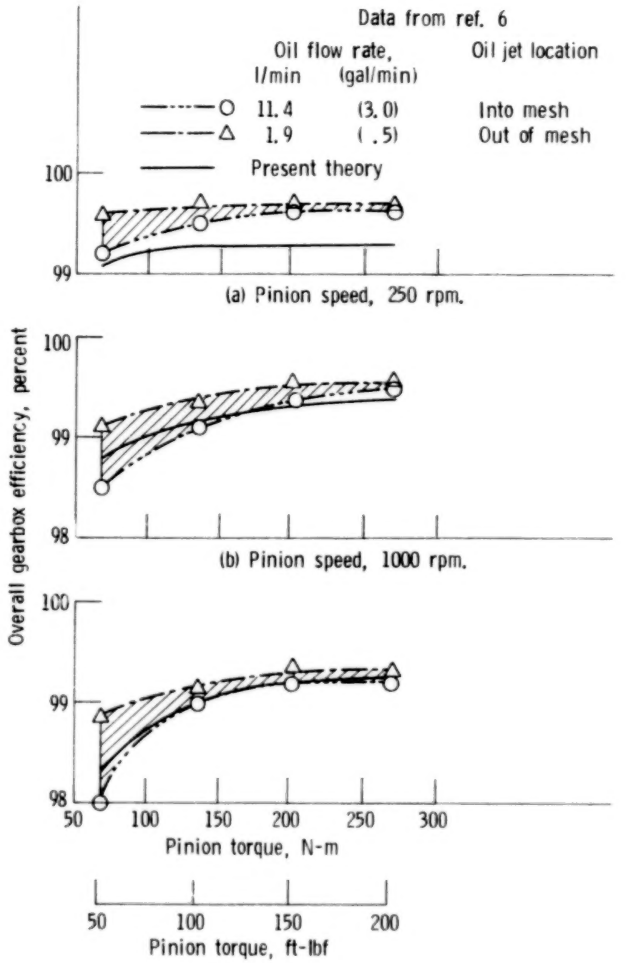

Figure 6. - Comparison of predicted overall gearbox efficiency with range of data from reference 6. Gear width, 4.0 centimeters (1.563 in.).

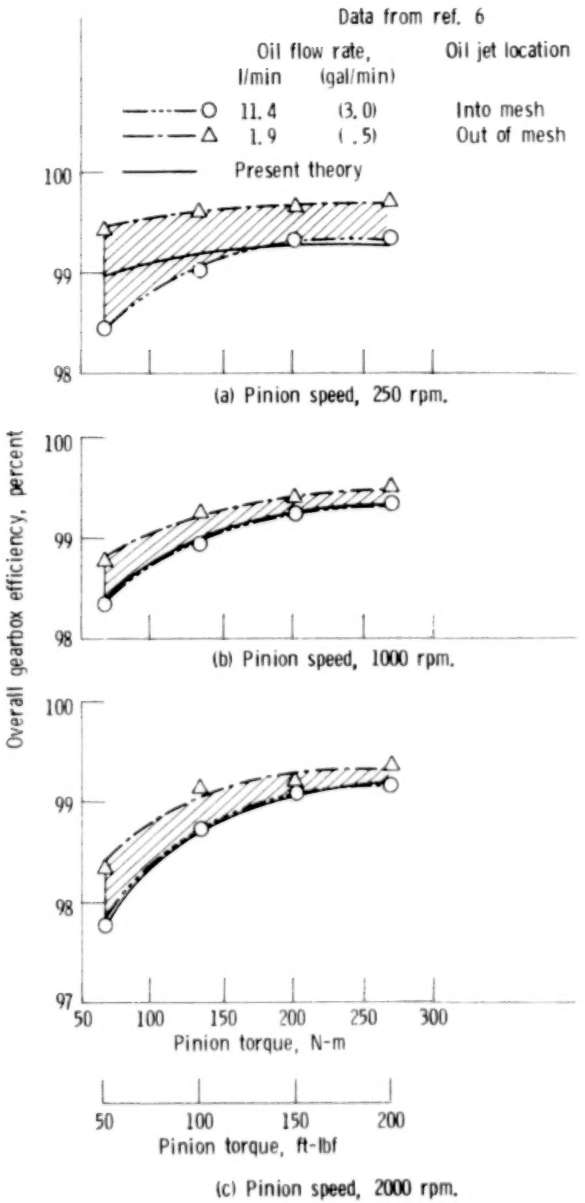

(a) Pinion speed, 250 rpm.

(b) Pinion speed, 1000 rpm.

(c) Pinion speed, 2000 rpm.

Figure 7. - Comparison of predicted overall gearbox efficiency with range of data from reference 6. Gear width, 7.94 centimeters (3.125 in.).

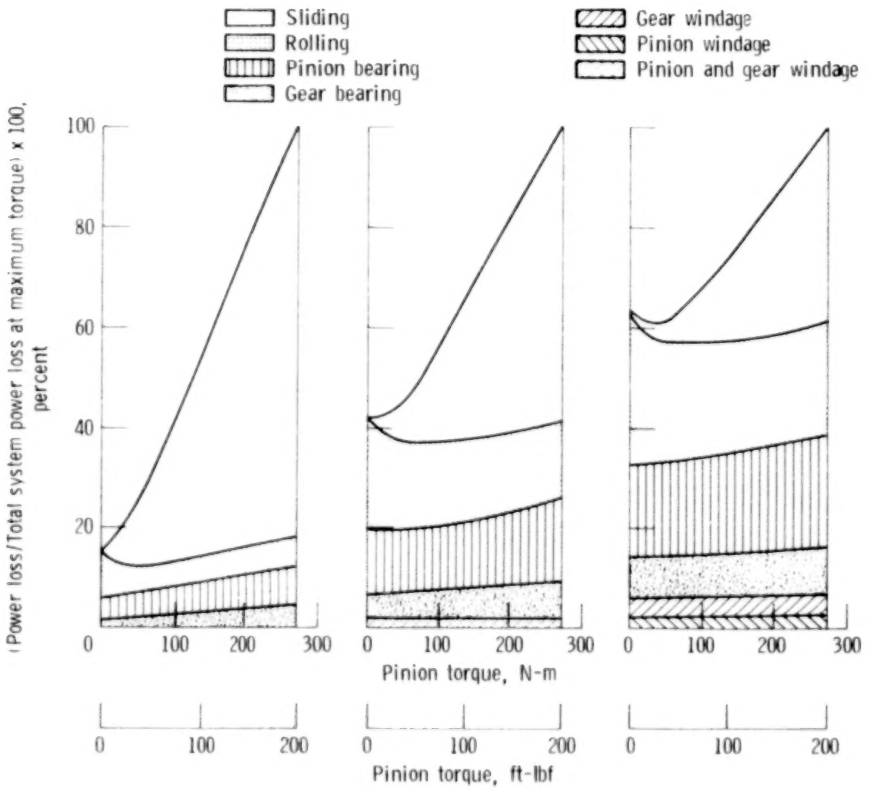

(a) Pinion speed, 250 rpm.

(b) Pinion speed, 1000 rpm.

(c) Pinion speed, 2000 rpm.

Figure 8. - Theoretical percentage comparison of sources of gearbox power loss as function of input torque for three pinion speeds. Gear width, 4.0 centimeters (1.563 in.); gear geometry and operating parameters given in table I.

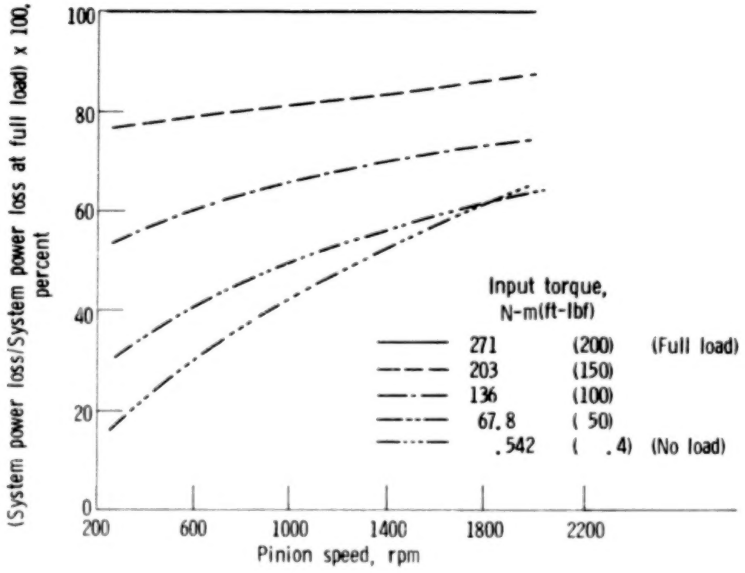

Figure 9. - Theoretical percentage of spur-gear-system power loss at part-load conditions relative to full-load power loss. Gear width, 4.0 centimeters (1.563 in.); gear geometry and operating parameters given in table I.

1. Report No. NASA TP-1622 AVRADCOM TR 79-46	2. Government Accession No.	3. Recipient's Catalog No.
4. Title and Subtitle SPUR-GEAR-SYSTEM EFFICIENCY AT PART AND FULL LOAD		5. Report Date February 1980 6. Performing Organization Code
7. Author(s) Neil E. Anderson and Stuart H. Loewenthal		8. Performing Organization Report No. E-061 10. Work Unit No. 505-04
9. Performing Organization Name and Address Propulsion Laboratory AVRADCOM Research and Technology Laboratories NASA Lewis Research Center Cleveland, Ohio 44135		11. Contract or Grant No. 13. Type of Report and Period Covered Technical Paper
12. Sponsoring Agency Name and Address National Aeronautics and Space Administration Washington, D.C. 20546 and U.S. Army Aviation Research and Development Command St. Louis, MO 63166		14. Sponsoring Agency Code

15. Supplementary Notes

Neil E. Anderson, AVRADCOM Research and Technology Laboratories; Stuart H. Loewenthal, Lewis Research Center.

16. Abstract

A simple method for predicting the part- and full-load power loss of a steel spur gearset of arbitrary geometry supported by ball bearings was developed. The analysis algebraically accounts for losses due to gear sliding, rolling traction, and windage in addition to support-ball-bearing losses. The analysis compared favorably with test data. A theoretical comparison of the component losses indicated that losses due to gear rolling traction, windage, and support bearings are significant and should be included along with gear sliding loss in a calculation of gear-system power loss.

17. Key Words (Suggested by Author(s))

Spur-gear efficiency
Efficiency
Power loss
Spur gear

18. Distribution Statement

Unclassified - unlimited
STAR Category 37

19. Security Classif. (of this report)	20. Security Classif. (of this page)	21. No. of Pages	22. Price*
Unclassified	Unclassified	40	A03

* For sale by the National Technical Information Service, Springfield, Virginia 22161

NASA-Langley, 1980

90 %

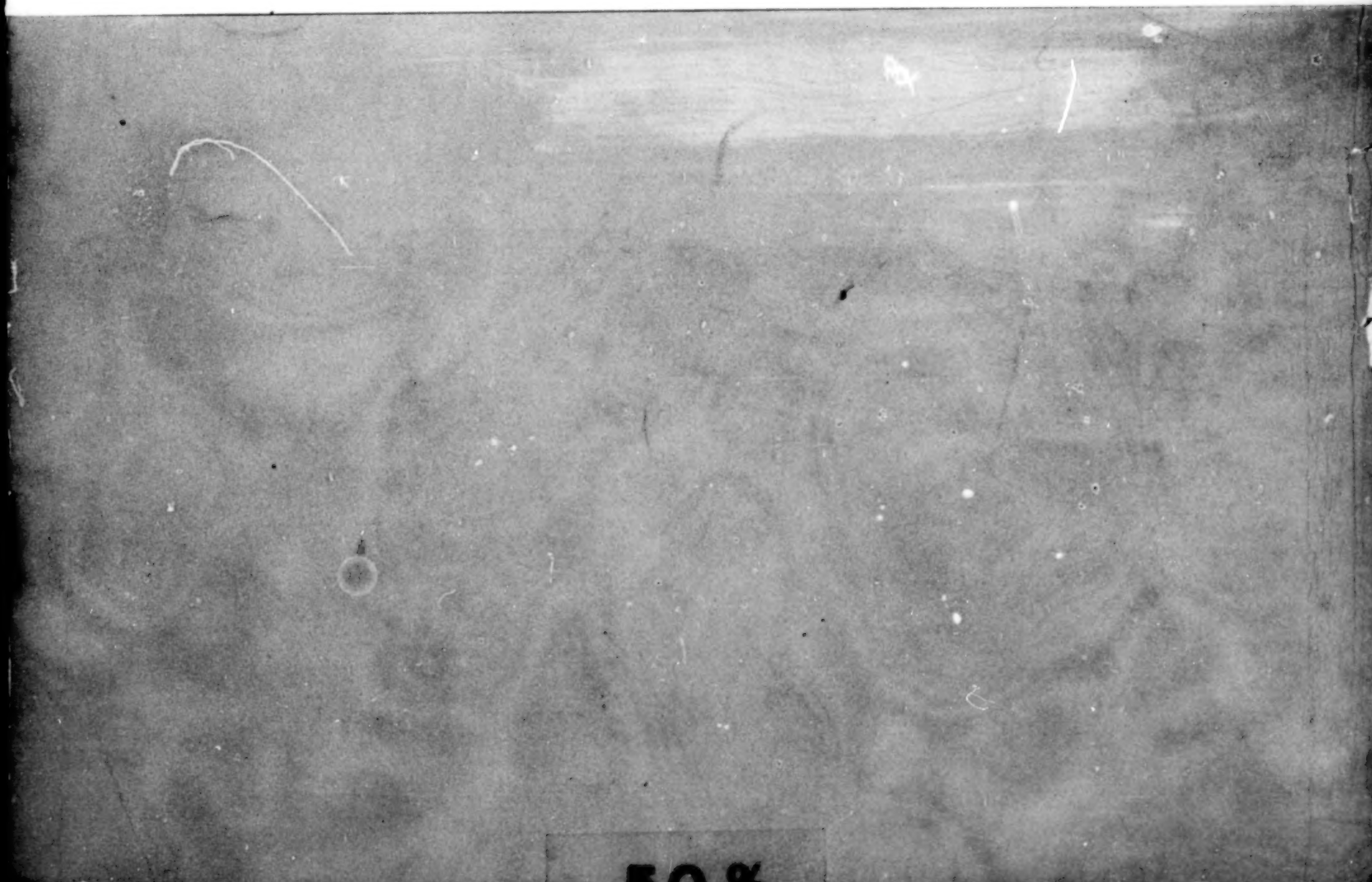

50 %